Binding of Madindoline A to the Extracellular Domain of gp130[†]

Abu Z. M. Saleh,[‡] Kevin L. Greenman,[§] Susan Billings,[§] David L. Van Vranken,[§,||] and John J. Krolewski*[,‡,||]

Department of Pathology, Department of Chemistry, and Chao Family Comprehensive Cancer Center, University of California, Irvine, California 92697

Received March 8, 2005; Revised Manuscript Received May 30, 2005

ABSTRACT: Elevated levels of IL-6 and IL-11 are associated with multiple myeloma, rheumatoid arthritis, hypercalcemia, cancer cachexia, and Castleman's disease. Madindoline A (MadA), isolated from *Streptomyces nitrosporeus* K93-0711, specifically inhibits the growth of IL-6- and IL-11-dependent cell lines, most likely by interfering with the homodimerization of gp130. This raises the possibility that MadA can be used as a model compound for the development of novel chemotherapeutic agents. In this report, we demonstrate that the binding of MadA to gp130 is specific and noncovalent, and displays a relatively low affinity. Furthermore, we show that the tricyclic 3a-hydroxytetrahydrofuro[2,3-*b*]indole (HFI) moiety of MadA alone is not sufficient for binding. Matrix-bound MadA precipitates a protein composed of the extracellular domain of gp130 fused to the Fc region of the immunoglobulin heavy chain. Binding is inhibited in a dose-dependent manner by preincubation with free MadA. The K_D for binding of MadA to gp130 is 288 μM, as determined by surface plasmon resonance (SPR)-based biosensor analysis. The HFI portion of MadA does not bind to gp130 in either affinity precipitation or SPR analyses. Finally, MadA, but not the HFI portion, inhibits IL-6-dependent Stat3 tyrosine phosphorylation in HepG2 cells.

The large family of α-helical cytokines (*1*) and the corresponding receptors are mediators of a wide variety of critical physiological functions regulating immune response, proliferation, differentiation, and apoptosis. The cytokine receptors share a common protein fold, termed the hematopoietin receptor domain, or cytokine-binding homology region, composed of two fibronectin type III domains (*2*). These receptors are divided into two classes or types, based upon amino acid sequence homologies with the cytokine-binding homology region. Within the type I cytokine receptor class, the largest subfamily is related to the membrane glycoprotein gp130. The best-characterized ligands for the gp130-related receptors include interleukin-6 (IL-6),[1] interleukin-11 (IL-11), leukemia inhibitory factor (LIF), oncostatin M, ciliary neurotrophic factor, and cardiotrophin-1 (*2*). The gp130 receptor protein is a common signal transducing receptor subunit for all these cytokines (*3*) and can be utilized either as a homodimer or as a heterodimer. IL-6 and IL-11 induce gp130 homodimerization, whereas the other members utilize gp130 as a heterodimer in conjunction with related ligand specific receptors. Ligand binding in all cases leads to the activation of the JAK/STAT signal transduction pathway (*4*). The JAK kinases are physically associated with the receptors. Ligand binding activates the JAK tyrosine kinases, resulting in receptor phosphorylation. Once phosphorylated, gp130 serves as a docking site for recruitment and subsequent tyrosine phosphorylation of Stat3 (*5*, *6*). Elevated levels of IL-6 have been observed in many cancers, particularly multiple myeloma and renal cell carcinomas (*7*). This cytokine has also been implicated in a variety of inflammatory conditions, including rheumatoid arthritis, Castleman's disease, and Crohn's disease (*8*).

Omura and colleagues have previously reported the isolation of metabolites from *Streptomyces nitrosporeus* K93-0711 that can selectively inhibit the growth of IL-6- and IL-11-dependent cell lines (*9*). Two of these natural products, madindoline A (MadA) and madindoline B (MadB), are diastereomers (Figure 1A,B), with MadA being the more potent with an IC_{50} 5-fold lower than that of MadB. Subsequently, it was shown that MadA inhibits IL-6 and IL-11 signaling and binds gp130, suggesting that MadA interferes with the homodimerization of this receptor protein (*10*). In this study, we further characterize the mechanism of MadA by demonstrating that it binds directly, but noncovalently, to the extracellular domain of gp130 and by determining the equilibrium dissociation constant for MadA with gp130 (280 μM). We also characterize the structural determinants of MadA that are required for binding to gp130.

EXPERIMENTAL PROCEDURES

Materials. The following antibodies were used in immunoblotting: rabbit anti-HA (Santa Cruz Biotechnology), at a 1:5000 dilution; mouse monoclonal anti-phospho-Stat3 (Y705) clone 9E12 (Upstate Biotechnology), at a 1:20000 dilution; and rabbit anti-Stat3 (Santa Cruz) antisera, at a 1:2000 dilution. Recombinant human IL-6 was from Pep-

[†] This work is supported by research grants from the National Institutes of Health (Grant CA056862 to J.J.K. and Grant GM54523 to D.L.V.V.).

* To whom correspondence should be addressed. E-mail: jkrolews@uci.edu. Telephone: (949) 8224-4089. Fax: (949) 824-2160.

[‡] Department of Pathology.

[§] Department of Chemistry.

[||] Chao Family Comprehensive Cancer Center.

[1] Abbreviations: IL-6, interleukin-6; IL-11, interleukin-11; LIF, leukemia inhibitory factor; MadA, (±)-madindoline A; MadB, (±)-madindoline B; IBA, indole(diazenyl)benzoic acid; LMadA, madindoline(diazenyl)benzoic acid; TG, Tentagel; HFI, 3a-tetrahydrofuro[2,3-*b*]indole; ECD, extracellular domain; SPR, surface plasmon resonance; CD5L, CD5 leader; RU, resonance units.

10.1021/bi050439+ CCC: $30.25
Published on Web 07/22/2005

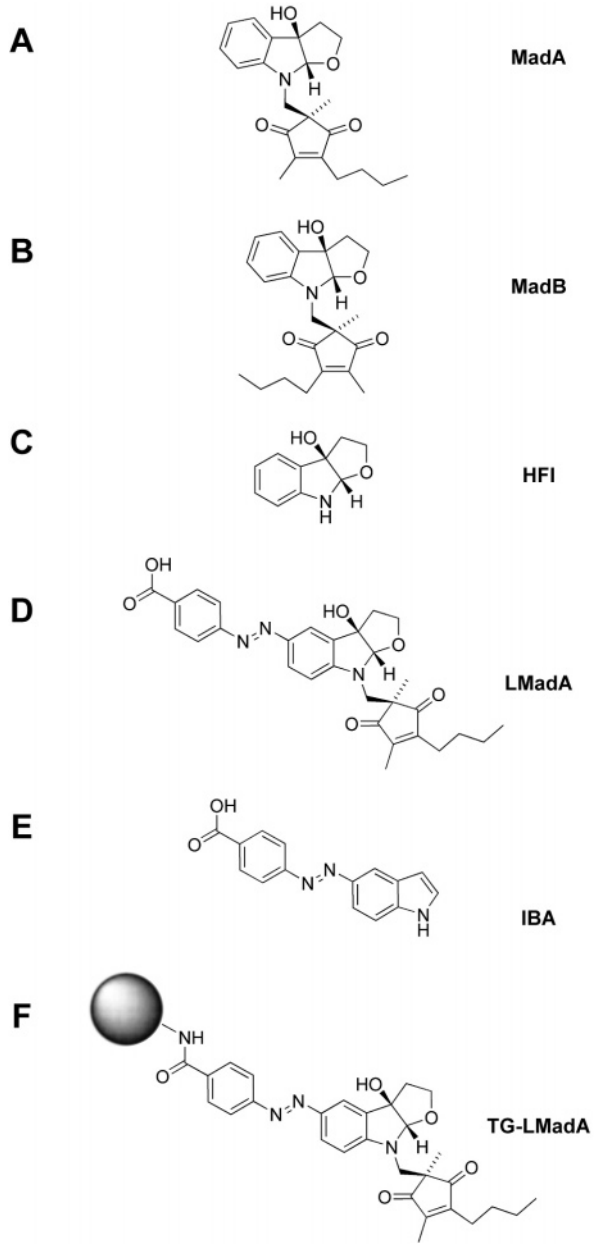

FIGURE 1: Chemical structure of madindolines and derivatives. The following structures are shown, with relative stereochemistry: (±)-madindoline A (MadA) (A), (±)-madindoline B (MadB) (B), 3a-hydroxytetrahydrofuro[2,3-*b*]indole (HFI) (C), MadA coupled to a (diazenyl)benzoic acid linker (LMadA) (D), 4-[2-(1*H*-indol-5-yl)-(diazenyl)]benzoic acid (IBA) (E), and LMadA coupled to the TentaGel bead matrix (TG-LMadA) (F).

rotech. The HEK293T cell line was from H. Young (College of Physicians and Surgeons, Columbia University, New York, NY), and the HepG2 cell line was from T. Osborne (University of California, Irvine, CA). HPLC-grade ethyl acetate, dichloromethane, methanol, hexanes, and acetonitrile were from E. M. Science. *N*,*N*′-Diisopropylcarbodiimide (DIC), *N*,*N*-dimethyl-4-aminopyridine (DMAP), and amino Tentagel S resin were purchased from Novabiochem.

Chemical Syntheses. MadA and MadB were synthesized as previously described (*11*). The (diazenyl)benzoic acid linker was installed by treating MadA (12 μmol) in acetonitrile (200 μL) at 0 °C with five portions of 4-carboxybenzenediazonium tetrafluoroborate (*12*) (60 μmol) at 15 min intervals. The mixture was stirred for a further 30 min and concentrated in vacuo, and the resulting residue was purified by flash chromatography (*13*). Elution with a 1:1 ethyl acetate/hexane mixture afforded unreacted MadA (5 μmol). Further elution with a 90:9:1 ethyl acetate/methanol/acetic acid mixture gave the madindoline(diazenyl)benzoic acid conjugate (LMadA) (6 μmol, 50% yield). The indole-(diazenyl)benzoic acid (IBA) molecule was prepared by reacting indole (85 μmol) with one portion of 4-carboxybenzenediazonium tetrafluoroborate (97 μmol) in acetonitrile (1 mL) at 0 °C for 30 min. The mixture was concentrated in vacuo and subjected to flash chromatography under the conditions described above to afford IBA (79 μmol, 93% yield). Immobilization onto TentaGel resin was accomplished by reacting madindoline(diazenyl)benzoic acid (4 μmol) with DIC (4 μmol in dichloromethane) in the presence of DMAP (4 μmol) at 0 °C in dichloromethane (1 mL). After 5 min, the TentaGel resin was added (19.6 mg) and the mixture stirred vigorously for 6 h. The resin was filtered over a medium sintered glass frit and washed with dichloromethane (3 × 10 mL), a 5% sodium bicarbonate solution (2 × 10 mL), water (2 × 10 mL) and methanol (3 × 10 mL). The final product (TG-LMadA) was dried in vacuo for 12 h. The immobilization of MadA onto TentaGel was judged to be quantitative. Therefore, no attempt was made to cap residual amines. IBA was coupled to TentaGel resin using the same procedure. The compound 3a-hydroxytetrahydrofuro[2,3-*b*]-indole (HFI) was synthesized as described previously (*11*).

Plasmid DNA Constructs. To amplify the extracellular domain (ECD) of gp130 (spanning amino acid residues 18−615), the corresponding cDNA was PCR amplified using *Pfu* polymerase (Stratagene) with the primers 5′-ACGCTAG-CAGAATCTACAGGTGAAC and 5′-TAGGATCCGCG-GCTTCAATTTCTC. The resulting 1.8 kB amplified DNA was sequenced, digested with *Nhe*I and *Bam*HI, and cloned into a modified Bluescript vector [derived from pCD5Lneg1 (*14*)] downstream of the CD5 leader (CD5L) sequence and upstream of a region encoding the human immunoglobulin heavy chain Fc domain. A 3.3 kb fragment containing the CD5L-gp130-ECD-Fc sequence was transferred into a version of the eukaryotic expression vector, pMT2T, so that an HA epitope tag was added to the extreme carboxyl terminus. A plasmid encoding CD5L-Fc-HA, downstream of the CD5L sequence, was constructed in a similar fashion.

Expression and Purification of Recombinant Proteins. Plasmid DNAs expressing Fc-HA and gp130-Fc-HA were separately transfected in the form of calcium phosphate precipitates into HEK293T cells (twelve 15-cm dishes containing 4 × 10^6 cells, for each construct). Forty-eight hours later, medium was collected, centrifuged to remove residual cells, adjusted to pH 8.0, and passed through a 0.45 μm filter. The medium was pumped through a 5 mL protein A column (Bio-Rad) which was washed successively with 50 mL of 100 mM Tris-HCl (pH 8.0) and then 50 mL of 10 mM Tris-HCl (pH 8.0). Bound protein was eluted with 25 mL of 100 mM glycine (pH 3.0) at a flow rate of 1 mL/min. Fractions were collected into 1.0 M Tris-HCl and analyzed by anti-HA immunoblotting. Fractions containing recombinant protein were pooled, dialyzed against HBS buffer [10 mM HEPES (pH 7.4), 0.15 M NaCl, 3 mM EDTA, and 0.005% P20], and concentrated by Centricon-30 (Amicon) centrifugation. Protein concentrations were determined using the Bradford reagent (Bio-Rad).

Affinity Precipitation and Immunoblotting. Purified gp130-Fc-HA recombinant protein was diluted to a final concentration of 12.8 nM in 150 μL of HBS buffer and incubated with 20 μL of TentaGel beads coupled to MadA or IBA, for 1 h at 4 °C with mixing. In some cases, gp130-ECD proteins were preincubated in the presence of free MadA or HFI for 1 h. The bound complexes were recovered by centrifugation, washed with HBS buffer, and eluted by heating them in sample buffer. SDS−PAGE, immunoblotting, and chemiluminescence detection were carried out as previously described (*15*).

Surface Plasmon Resonance Analysis. Surface plasmon resonance (SPR) analysis was performed using a model 3000 Biosensor (BIAcore). Recombinant gp130-Fc-HA and Fc-HA proteins were cross-linked to two different flow cells on a dextran matrix of a CM5 sensor chip (BIAcore) using standard amino group coupling methods according to the manufacturer's instructions. Approximately 5000 resonance units (RU) of gp130-Fc-HA and Fc-HA were cross-linked to each flow cell. For the equilibrium analysis, various concentrations of MadA (or MadB or HFI) were injected for a period of 2 min at a flow rate of 30 μL/min, in series, into flow cells containing Fc-HA (reference flow cell) and gp130-Fc-HA. Bound ligand (MadA) was removed by passing 0.5% SDS over the chip surface. The steady-state equilibrium response (RU_{eq}) was determined from the reference-subtracted sensorgrams using BIA Evaluation 2.1 (Pharmacia) and subjected to Scatchard analysis for calculation of the K_D (equilibrium dissociation constant).

RESULTS

Purification of the Recombinant gp130 Extracellular Domain. Omura and colleagues (*10*) demonstrated that MadA blocked the cellular effects of IL-6 and IL-11 but not related cytokines such as LIF, suggesting that MadA acts by inhibiting one or more of the functions of gp130. Furthermore, MadA did not inhibit G-CSF-induced proliferation of BAF cells expressing a chimeric receptor consisting of the extracellular domain of the G-CSF receptor and the intracellular domain of gp130, apparently narrowing the target of MadA to the extracellular domain of gp130. To determine if MadA binds directly to the extracellular domain of gp130, we generated a fusion between this region and the Fc domain of the immunoglobulin heavy chain. The signal sequence from CD5 was included at the amino terminus to facilitate secretion of the fusion protein, and an HA epitope tag was added to the extreme carboxyl terminus (Figure 2A). This chimeric protein (gp130-Fc-HA) was expressed in HEK293T cells and purified by protein A affinity chromatography from the medium of transfected cells, as described in Experimental Procedures (Figure 2B). Immunoblotting with an anti-HA antibody confirmed that the major species corresponded to the predicted fusion protein (Figure 2C).

The Extracellular Domain of gp130 Binds Directly to MadA. To examine the physical association between the extracellular domain of gp130 and MadA, we first synthesized a (diazenyl)benzoic acid-linked version of MadA (Figure 1D) and coupled this to Tentagel beads (Figure 1F). These beads affinity precipitated purified gp130-Fc-HA, indicating that the extracellular domain of gp130 binds MadA directly (Figure 3). Purified Fc-HA was not precipitated by

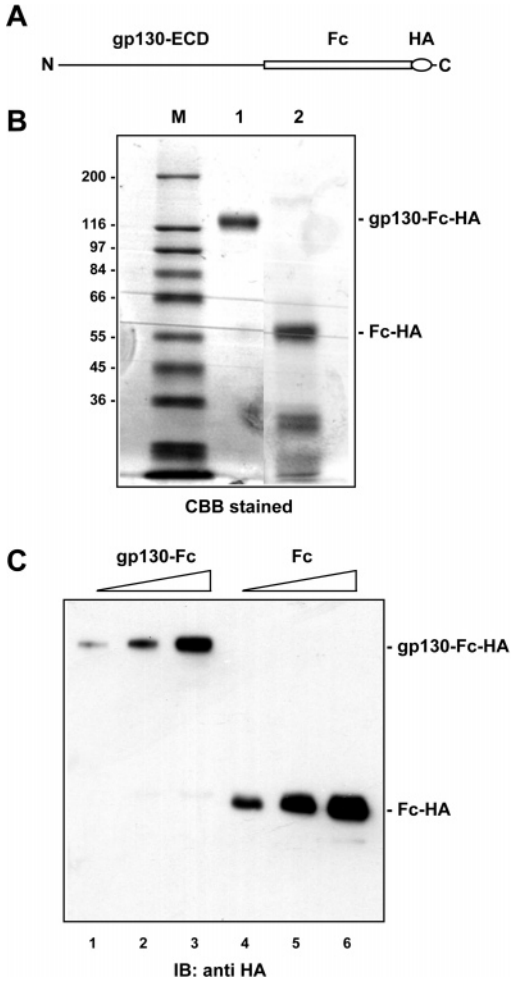

FIGURE 2: Purification of recombinant gp130-Fc protein. (A) Structure of recombinant gp130-Fc-HA. ECD corresponds to the extracellular domain of gp130 (amino acids 18−615), Fc to amino acids 236−467 of the human immunoglobulin heavy chain, and HA to the hemagglutinin epitope tag. (B) Coomassie Blue-stained gel of the purified proteins: lane M, molecular weight standards; lane 1, gp130-Fc-HA (5.7 μg); and lane 2, Fc-HA (3.5 μg). (C) Anti-HA immunoblot of the purified proteins: lanes 1−3, gp130-Fc-HA (0.38, 0.77, and 1.54 μg, respectively); and lanes 4−6, Fc-HA (0.12, 0.24, and 0.48 μg, respectively).

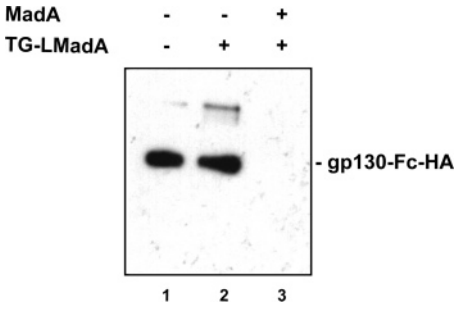

FIGURE 3: In vitro binding of MadA to the extracellular domain of gp130. Purified gp130-Fc-HA recombinant protein (12.8 nM) preincubated in the absence (lane 2) or presence (lane 3) of free MadA (1.25 mM) was reacted with TG-LMadA for 1 h, and the resulting complex was recovered and immunoblotted with an anti-HA antibody. Lane 1 contained recombinant gp130-Fc (10% of the amount used in the binding assays).

TG-LMadA (data not shown). Preincubation of gp130-Fc-HA with 1.1 mM free MadA completely inhibited the binding of gp130 to TG-LMadA (Figure 3, lane 3). Figure 4 demonstrates that such preincubation with free MadA has a

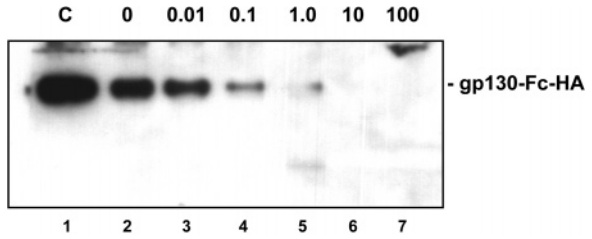

FIGURE 4: Free MadA inhibits binding of TG-LMadA to gp130. Aliquots of gp130-Fc-HA (12.8 nM) were incubated with free MadA at various concentrations (lanes 2−7, concentration in micromolar, as indicated) for 30 min, followed by the addition of TG-LMadA. After 1 h, complexes were recovered and immunoblotted with an anti-HA antibody. Lane 1 contained recombinant gp130-Fc only (20% of the amount used in the binding assays).

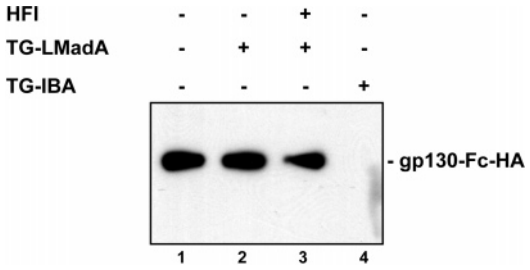

FIGURE 5: HFI does not bind gp130. As in Figure 4, recombinant gp130-Fc-HA (12.8 nM) was preincubated with HFI (100 μM) for 30 min or left untreated, as indicated. TG-LMadA (lanes 2 and 3) or TG-IBA (lane 4) was added; the incubation was continued for an additional 1 h, and the complexes were recovered and immunoblotted with an anti-HA antibody. Lane 1 contained recombinant gp130-Fc-HA only (10% of the amount used in the binding assays).

dose-dependent effect on the subsequent binding of gp130 to TG-LMadA. Specifically, a free MadA concentration as low as 100 nM significantly inhibited the affinity precipitation of gp130-Fc-HA by TG-LMadA (Figure 4, lane 4). Although we have previously suggested the possibility that MadA could covalently interact with cysteine thiol groups (*11*), Figures 3 and 4 are consistent with a noncovalent interaction since gp130-Fc-HA is released from the TG-LMadA beads after 3 min at 95 °C in sample buffer (2% SDS and 5% 2-mercaptoethanol).

The Tricyclic Indole Moiety of MadA Is Not Sufficient for gp130 Binding. The affinity precipitation of gp130-Fc-HA by TG-LMadA (Figures 3 and 4) indicates that a major substitution on the tricyclic 3a-tetrahydrofuro[2,3-*b*]indole (HFI; Figure 1C) moiety of MadA does not preclude binding. To further investigate the role of this tricyclic moiety, gp130-Fc-HA was preincubated with 100 μM HFI prior to affinity precipitation using TG-LMadA, in an experiment similar to that shown in Figure 3. Figure 5 (lanes 2 and 3) demonstrates that preincubation with HFI did not affect binding of gp130 to MadA, suggesting that this portion of the molecule is insufficient for binding. The indole portion of the tricyclic moiety was also coupled via the (diazenyl)benzoic acid linker (Figure 1E) to Tentagel beads (HFI was not employed in this case because it could not be efficiently coupled). This control molecule was not able to affinity precipitate gp130-Fc-HA (Figure 5, lane 4).

Surface Plasmon Resonance Measurement of the K_D for Binding of MadA to gp130-ECD. To determine the equilibrium dissociation constant (K_D) for the interaction of MadA with the gp130 extracellular domain, we employed surface plasmon resonance-based biosensor analysis. Purified gp130-Fc-HA was covalently cross-linked to the dextran matrix of a CM5 sensor chip. Subsequently, various concentrations of MadA were injected over this surface (as well as a reference surface containing only the dextran matrix), and the interaction was monitored in real time. Figure 6A shows overlaid plots of a series of reference-subtracted sensorgrams corre-

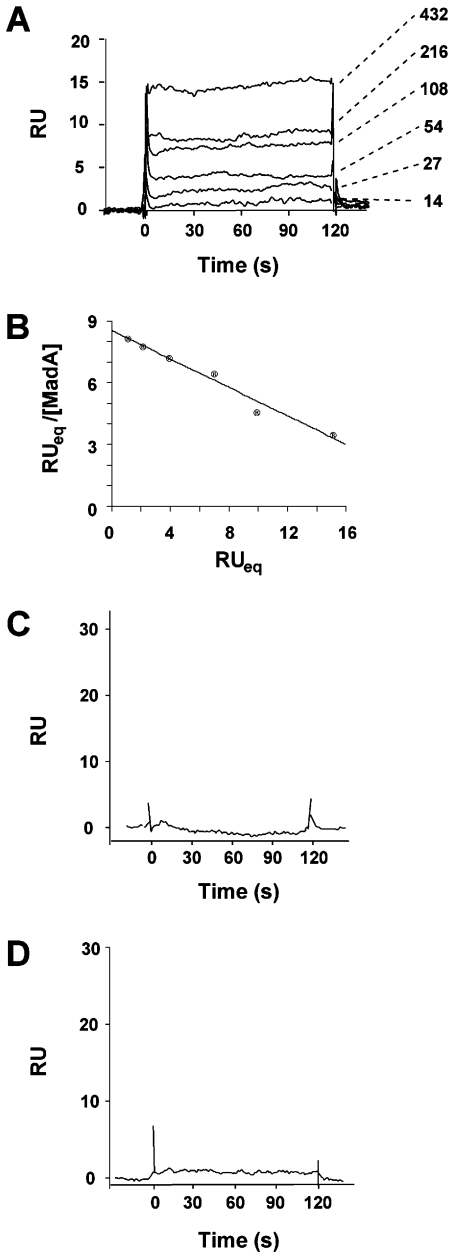

FIGURE 6: SPR biosensor analysis of the interaction of MadA with gp130-Fc-HA. (A) SPR sensorgrams. Purified gp130-Fc was covalently cross-linked to a CM5 sensor chip, and MadA was sequentially passed over the cross-linked chip and a reference chip, as described in Experimental Procedures. Reference-subtracted sensorgrams corresponding to MadA at increasing concentrations (as indicated, in micromolar) are plotted as overlays. (B) Scatchard analysis. Steady-state equilibrium binding responses (RU_{eq}) were determined from panel A and plotted as shown. The K_D (288 μM) was determined from the slope of the plot. A replicate of the SPR binding seen in Figure 6A generated a K_D of 192 μM, with an R^2 of 0.92 for the linear curve fitting of the Scatchard plot (the R^2 value for the data set shown is 0.97). (C) SPR sensorgram of the interaction of gp130-Fc-HA with MadB. Like panel A except MadB (600 μM) was substituted for MadA. (D) SPR sensorgram of the interaction of gp130-Fc-HA with HFI. Like panel A except HFI (600 μM) was substituted for MadA.

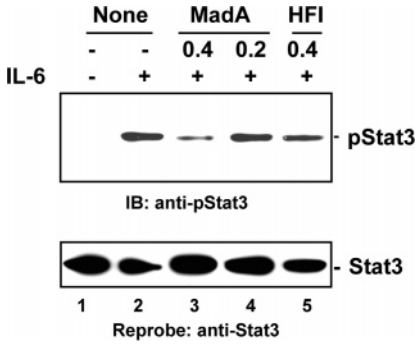

FIGURE 7: MadA inhibits IL-6-dependent tyrosine phosphorylation of Stat3. HepG2 cells (2.5×10^6 cells) were pretreated for 30 min with MadA or HFI at the indicated concentration (millimolar) or left untreated (None) and then treated with recombinant human IL-6 (0.6 μg/mL) for an additional 30 min (or left untreated). Lysates were immunoblotted with anti-phospho-Stat3 antibody (top panel). The same filter was stripped and reprobed with anti-Stat3 antibody (bottom panel).

sponding to binding performed at progressively increasing concentrations of MadA. The RU_{eq} values derived from the sensorgrams were used in a Scatchard analysis (Figure 6B) to calculate a K_D of 288 μM for the MadA−gp130 interaction, assuming a 1:1 drug:receptor stoichiometry. In control experiments, MadB (Figure 1B) and HFI were injected in place of MadA. No binding to gp130-ECD was observed in either case (Figure 6C,D), indicating that the binding of MadA to the extracellular domain of gp130 is specific.

MadA, but Not HFI, Inhibits IL-6-Dependent Tyrosine Phosphorylation of Stat3. Hayashi and colleagues (*10*) previously demonstrated that MadA blocked the ability of IL-6 to induce tyrosine phosphorylation of Stat3. Figure 7 confirms this observation, demonstrating that 400 μM MadA inhibits Stat3 tyrosine phosphorylation (lane 2 vs lane 3). Figure 7 also shows that a similar concentration of HFI, which did not show significant binding to gp130 (Figure 5), has an only slight effect on Stat3 phosphorylation in response to IL-6 (lane 2 vs lane 6).

DISCUSSION

MadA is a noncytotoxic natural product that appears to specifically inhibit signaling by the IL-6 and IL-11 cytokines, but not closely related cytokines such as LIF. Given this relatively restricted target specificity, MadA has potential utility as a model or lead compound for future drug development aimed at a number of neoplastic and inflammatory conditions which are characterized by elevated levels of these particular cytokines. Omura and colleagues employed bioassays using cell lines expressing either endogenous cytokine receptors or artificial chimeric receptors to functionally assign the site of action of MadA to the extracellular domain of the gp130 receptor subunit (*9*, *10*). They also observed that radiolabeled MadA can bind to gp130 in an immunoblot "overlay" assay. However, it is unclear from this initial data whether MadA binds covalently or noncovalently, precisely which gp130 domains are required for binding, and how strongly MadA binds gp130.

To address these questions, and to further characterize the biochemical mechanism of MadA action, we developed two useful molecular reagents: a recombinant protein in which the extracellular domain of gp130 was fused to the Fc portion of the immunoglobulin heavy chain (Figure 2) and a version of MadA coupled to TentaGel beads via a linker attached to the 5-position of the indole ring (Figure 1F). The use of a signal sequence to ensure secretion into the medium and the presence of the Fc domain facilitated purification of gp130-Fc to apparent homogeneity via a one-step protein A affinity chromatography procedure (Figure 2). Affinity precipitation of this recombinant protein thus demonstrates that binding of MadA to gp130 is direct and requires only the extracellular domain (Figures 3 and 4). Thus, we are able to confirm the prediction based on functional studies that MadA binds directly to the gp130 extracellular domain. Furthermore, since we are able to release the bound gp130-Fc from the MadA-linked beads under standard denaturing conditions, it is highly likely that the MadA−gp130 interaction is noncovalent. In particular, cleavage of the linker from the resin (amide bond hydrolysis) and cleavage of the linker from madindoline (azo bond hydrolysis) are improbable mechanisms for release of the matrix-bound protein into solution under the conditions that were employed. However, a covalent interaction cannot be rigorously ruled out.

Our studies also provide significant insight into the structural features of the MadA molecule that are required for interaction with gp130. On the basis of the observations (i) that addition of the diazenylbenzoic acid linker to the tricyclic HFI ring does not preclude affinity precipitation in Figures 3−5 and (ii) that the tricyclic indole ring structure does not bind gp130 (Figure 6) or competitively inhibit MadA binding (Figures 5 and 7), we can conclude that the "top half" of MadA alone is not sufficient for binding. This further suggests that the "bottom half" of MadA (containing a diketo cyclopentene moiety) is required for binding to gp130. It remains to be determined if the bottom half functions synergistically with the top half, or if the bottom half is entirely sufficient for binding.

The SPR data in Figure 6 predict that the K_D for the MadA−gp130 interaction is ~300 μM. This is consistent with the data in Figure 7, which indicates that 50% inhibition of Stat3 tyrosine phosphorylation occurs at a MadA concentration between 200 and 400 μM. The data in Figure 4 are derived from preincubation of MadA with gp130-Fc-HA and thus cannot be reliably used to determine the binding affinity. It has been previously reported that the IC_{50} of MadA in cell proliferation studies is ~70 μM (*10*). In addition, these same authors report that a lower concentration of MadA (100 μM) was quite effective in inhibiting IL-6-dependent Stat3 tyrosine phosphorylation. Half of this approximately 4-fold difference in apparent affinity can be attributed to differences in madindoline preparations. In contrast to the preparations used by Omura and colleagues, the preparation we used is racemic [i.e., contains both (+) and (−) enantiomers]. Therefore, the concentration of (+)-madindoline A is half the concentration of the racemic MadA preparation we used, bringing our data into reasonably close agreement with previously published studies. The similarity between the SPR-determined K_D and the approximate IC_{50} for Stat3 tyrosine phosphorylation derived from the immunoblot data of Figure 7 suggests that our biochemical binding experiments are good approximations of the in vivo mechanism of action for MadA. While the K_D value we have determined suggests that MadA is unlikely to be an effective therapeutic compound, the high degree of cytokine specificity observed

by Hayashi et al. (*10*) indicates that MadA may be potentially useful in the design of higher-affinity compounds that act similarly.

As noted in the introductory section, signaling by both IL-6 and IL-11 is mediated by gp130 homodimerization. Both of these cytokines also require an additional receptor protein (IL6-Rα, in the case of IL-6) which functions as a coligand (*3*). These three proteins (IL-6, IL-6Rα, and gp130) form a hexameric complex to initiate signaling (*16*). Functional (*17*, *18*) and structural studies (*16*, *19*) have made it clear that the key difference between IL-6 and LIF is that the former interacts with the D1 domain in gp130. In contrast, the D1 domain is superfluous for LIF, which signals via a heterodimer containing the LIF receptor and gp130. Since functional studies indicate that MadA inhibits IL-6 signaling but not LIF signaling, and since we have demonstrated that MadA binds to the extracellular domain of gp130, it is likely that the ultimate target of MadA is within the D1 domain. Our biochemical studies suggest that MadA binds to a monomeric form of gp130. This would be consistent with the hypothesis that MadA interferes with the interaction between a single gp130 D1 domain and the corresponding binding surface on a single IL-6 (or IL-11) molecule (*16*). Additional studies are required to determine if indeed the D1 domain is the target of MadA and to better understand the precise molecular interactions that determine binding specificity. The availability of linked MadA and recombinant gp130-Fc proteins will facilitate such studies by allowing us to rapidly test both mutagenized gp130 molecules and modifications of the MadA structure. This may lead to the design of novel compounds with increased affinity for gp130 and therefore potential therapeutic efficacy.

ACKNOWLEDGMENT

We thank H. Young and T. Osborne for providing cell lines and Duy Nguyen and Pasha Ehsan for assistance with the protein purifications.

REFERENCES

1. Bazan, J. F. (1990) Structural design and molecular evolution of a cytokine receptor superfamily, *Proc. Natl. Acad. Sci. U.S.A. 87*, 6934−6938.
2. Boulay, J. L., O'Shea, J. J., and Paul, W. E. (2003) Molecular phylogeny within type I cytokines and their cognate receptors, *Immunity 19*, 159−163.
3. Heinrich, P. C., Behrmann, I., Haan, S., Hermanns, H. M., Muller-Newen, G., and Schaper, F. (2003) Principles of interleukin (IL)-6-type cytokine signalling and its regulation, *Biochem. J. 374*, 1−20.
4. Lutticken, C., Wegenka, U. M., Yuan, J., Buschmann, J., Schindler, C., Ziemiecki, A., Harpur, A. G., Wilks, A. F., Yasukawa, K., Taga, T., Kishimoto, T., Barbieri, G., Pellegrini, S., Sendtner, M., Heinrich, P. C., and Horn, F. (1994) Association of transcription factor APRF and protein kinase JAK1 with the interleukin-6 signal transducer gp130, *Science 263*, 89−92.
5. Stahl, N., Farruggella, T. J., Boulton, T. G., Zhong, Z., Darnell, J. E., and Yancopoulos, G. D. (1995) Choice of STATs and other substrates specified by modular tyrosine-based motifs in cytokine receptors, *Science 267*, 1349−1353.
6. Hirano, T., Ishihara, K., and Hibi, M. (2000) Roles of STAT3 in mediating the cell growth, differentiation and survival signals through the IL-6 family of cytokine receptors, *Oncogene 19*, 2548−2556.
7. Trikha, M., Corringham, R., Klein, B., and Rossi, J. F. (2003) Targeted anti-interleukin-6 monoclonal antibody therapy for cancer: A review of the rationale and clinical evidence, *Clin. Cancer Res. 9*, 4653−4665.
8. Nishimoto, N., and Kishimoto, T. (2004) Inhibition of IL-6 for the treatment of inflammatory diseases, *Curr. Opin. Pharmacol. 4*, 386−391.
9. Omura, S., Hayashi, M., and Tomado, H. (1999) Recent progress of the research on novel microbial metabolites, *Pure Appl. Chem. 71*, 1673−1681.
10. Hayashi, M., Rho, M. C., Enomoto, A., Fukami, A., Kim, Y. P., Kikuchi, Y., Sunazuka, T., Hirose, T., Komiyama, K., and Omura, S. (2002) Suppression of bone resorption by madindoline A, a novel nonpeptide antagonist to gp130, *Proc. Natl. Acad. Sci. U.S.A. 99*, 14728−14733.
11. McComas, C. C., Perales, J. B., and Van Vranken, D. L. (2002) Synthesis of madindolines and chemical models. Studies of chemical reactivity, *Org. Lett. 4*, 2337−2340.
12. Kizil, M., Yilmaz, E. I., Pirinccioglu, N., and Aytekin, C. (2003) DNA cleavage activity of diazonium salts: chemical nucleases, *Turk. J. Chem. 27*, 539−544.
13. Still, W. C., Kahn, M., and Mitra, A. (1978) Rapid chromatographic technique for preparative separations with moderate resolution, *J. Org. Chem. 43*, 2923−2925.
14. Zettlmeissl, G., Gregersen, J.-P., Duport, J. M., Mehdi, S., Reiner, G., and Seed, B. (1990) Expression and characterization of human CD4: Immunoglobulin fusion protein, *DNA Cell Biol. 9*, 347−353.
15. Nguyen, V.-P., Saleh, A. Z. M., Arch, A. E., Yan, H., Piazza, F., Kim, J., and Krolewski, J. J. (2002) Stat2 binding to the interferon α receptor 2 (IFNaR2) subunit is not required for interferon-α signaling, *J. Biol. Chem. 277*, 9713−9721.
16. Boulanger, M. J., Chow, D. C., Brevnova, E. E., and Garcia, K. C. (2003) Hexameric structure and assembly of the interleukin-6/IL-6 α-receptor/gp130 complex, *Science 300*, 2101−2104.
17. Timmermann, A., Pflanz, S., Grotzinger, J., Kuster, A., Kurth, I., Pitard, V., Heinrich, P. C., and Muller-Newen, G. (2000) Different epitopes are required for gp130 activation by interleukin-6, oncostatin M and leukemia inhibitory factor, *FEBS Lett. 468*, 120−124.
18. Hammacher, A., Richardson, R. T., Layton, J. E., Smith, D. K., Angus, L. J., Hilton, D. J., Nicola, N. A., Wijdenes, J., and Simpson, R. J. (1998) The immunoglobulin-like module of gp130 is required for signaling by interleukin-6, but not by leukemia inhibitory factor, *J. Biol. Chem. 273*, 22701−22707.
19. Boulanger, M. J., Bankovich, A. J., Kortemme, T., Baker, D., and Garcia, K. C. (2003) Convergent mechanisms for recognition of divergent cytokines by the shared signaling receptor gp130, *Mol. Cell 12*, 577−589.

BI050439+